



Imaging modalities (MRI, CT, PET/CT), indications, differential diagnosis and imaging characteristics of cystic mediastinal masses: a review

Amar Shah, Carlos A. Rojas

Department of Radiology, Mayo Clinic in Arizona, Phoenix, AZ, USA

Contributions: (I) Conception and design: Both authors; (II) Administrative support: Both authors; (III) Provision of study materials or patients: Both authors; (IV) Collection and assembly of data: Both authors; (V) Data analysis and interpretation: Both authors; (VI) Manuscript writing: Both authors; (VII) Final approval of manuscript: Both authors.

Correspondence to: Carlos A. Rojas, MD. Department of Radiology, Mayo Clinic in Arizona, Phoenix, AZ, USA. Email: Rojas.carlos@mayo.edu.

Abstract: Cystic mediastinal masses have traditionally represented a diagnostic dilemma with differentiation of malignant masses a particular area of concern. Each imaging modality has strengths and weaknesses in mediastinal imaging—computed tomography (CT) offers increased spatial resolution at the cost of poorer soft tissue differentiation and requiring ionizing radiation, while magnetic resonance imaging (MRI) offers superior soft tissue contrast/characterization at significantly greater cost. Ultrasound offers real-time visualization but is operator and tissue dependent. [18F]fluoro-D-glucose (F-18 FDG) positron emission tomography (F-18 FDG PET) CT provides functional information, but poorer spatial resolution. Recent advances have focused upon the use of magnetic resonance imaging to aid in characterization of cystic mediastinal lesions, particularly in the context of indeterminate CT findings. The mediastinum may be divided into three anatomic compartments: prevascular, visceral, and paravertebral. All three compartments extend superiorly from the thoracic inlet and inferiorly to the diaphragm. These compartments provide a useful framework for categorizing normal and pathologic mediastinal processes. In this article, we will review the imaging characteristics of mediastinal cystic lesions via a case-based review divided by anatomical mediastinal compartments. Characteristic imaging features and troubleshooting are particular areas of focus. Normal variants that may mimic cystic pathology are discussed. The roles of CT and MRI will be emphasized. Cases from our institution are presented as illustrative examples.

Keywords: Mediastinum; magnetic resonance imaging (MRI); computed tomography (CT); ultrasound; cystic lesions

Received: 03 August 2022; Accepted: 25 November 2022; Published online: 26 December 2022.

doi: 10.21037/med-22-31

View this article at: <https://dx.doi.org/10.21037/med-22-31>

Introduction

Mediastinal cystic lesions are typically well-marginated, rounded or oval shaped lesions filled with fluid and lined with epithelium. While most mediastinal cystic masses are benign (duplication cysts, pericardial cysts, thymic cysts, teratomas, meningoceles, lymphangiomas, etc.), several tumors may initially present with a cystic component or undergo cystic degeneration, including lymphoma, thymoma, teratoma and nodal metastases.

The differential diagnosis of cystic mediastinal lesions

can be divided by location using the tricompartamental definition by Carter *et al.* and the International Thymic Malignancy Interest Group using cross-sectional imaging (1). This mediastinal compartment classification divides the mediastinum into three compartments: the prevascular compartment, the visceral compartment, and the paravertebral compartment. All three compartments extend superiorly from the thoracic inlet and inferiorly to the level of the diaphragm. The prevascular compartment includes all structures posterior to the sternum and anterior to the pericardium. The visceral compartment includes all

structures from the posterior boundary of the pre-vascular mediastinum to a vertical line connecting each thoracic vertebral body 1 cm posterior to their anterior margins. The paravertebral compartment includes all structures posterior to the posterior boundary of the visceral compartment to a vertical line along the posterior margin of the chest wall at the lateral margin of the transverse process of the thoracic spine.

Depending on the content of the cyst (simple fluid, protein, or blood products) imaging characteristics on computed tomography (CT) and magnetic resonance imaging (MRI) will vary. Often, lesions in the mediastinum have density above water ranging between 20 and 100 Hounsfield units (HU) and are therefore inconclusive for solid lesions versus complicated cysts. MRI is essential to distinguish solid from cystic lesions as well as for the evaluation of septations or solid components. Differentiation of benign and malignant lesions can be challenging. In addition to a thorough clinical history and physical examination, familiarity with the imaging patterns of mediastinal cysts is critical to differentiating benign and malignant lesions.

Imaging modalities

Role of CT

CT is often the modality by which mediastinal lesions are first identified and characterized. Characteristics of simple cysts on CT include low density (0 to 20 HU), thin (imperceptible) walls, few or no septations, and lack of contrast enhancement. CT provides two major advantages over MRI and US, namely rapid acquisition, and excellent spatial resolution of mediastinal structures. However, soft tissue contrast is poor, and identification of lesion margins can be difficult, even in contrast-enhanced studies. Cystic lesions (proteinaceous, infected, or hemorrhagic) in the mediastinum can be misinterpreted as solid due to cellular debris or blood products with resultant internal densities ranging between 20 and 100 HU. Masses with dense calcifications may obscure underlying soft tissue detail due to blooming artifact. Enhancing septations, indicative of increased vascularity, may be a herald of malignancy. Dual-energy CT with intravenous contrast can help differentiate cystic from solid lesions with material decomposition techniques using digital subtraction of iodine (intravenous contrast). This allows differentiation of tissue enhancement from hemorrhagic/proteinaceous fluid as well as differentiation of calcium from contrast accumulation.

Although there is scarcity of literature regarding the use of this technique in the evaluation of mediastinal masses, it is likely to play an important role in characterization of mediastinal lesions in the future.

Role of MRI

Magnetic resonance imaging is a key problem-solving tool for the characterization of mediastinal cystic masses. Unlike CT, MRI can more clearly characterize soft tissue lesions and identify infiltrative disease. Diffusion weighted imaging can identify lesions mimicking cysts, as cellular content/debris will cause diffusion restriction in comparison to simple cysts, which will not. Gadolinium contrast further allows characterization of lesion vascularity and enhancement. In and out of phase imaging allows identification of microscopic fat which is commonly seen in normal or hyperplastic thymic tissue. While MRI does not expose the patient to ionizing radiation, its cost and increased acquisition times are a drawback.

MRI is the preferred next step after an indeterminate CT, particularly to determine enhancement, identification of microscopic fat, and visualization of fine soft tissue detail (nodularity, septations). For example, MRI can readily differentiate hyperdense cysts from solid masses. In addition, when calcifications cause obscuring hyperdensity on CT, MRI will be unaffected. In various clinical scenarios, characteristic MR findings can make a certain diagnosis without the need for tissue sampling.

Strengths of MRI include differentiation between cystic and solid lesions, evaluation of simple versus complex cystic lesions, evaluation for restricted diffusion (seen on infection due to high cellular debris), and evaluation for the presence of blood products or contrast enhancement. As with CT, enhancing (vascular) septations can be a sign of malignancy. Furthermore, due to its high tissue contrast, invasion of adjacent soft tissue structures is well evaluated with MRI.

MRI of the mediastinum should, at a minimum, include in-and-out of phase T1, T1 weighted pre-and-post contrast, T2 weighted, and diffusion weighted sequences (2,3). Simple cysts will demonstrate smooth, thin walls with internal T1 hypointensity, T2 hyperintensity, and no diffusion restriction or contrast enhancement. Benign cysts may demonstrate intermediate or T1 hyperintensity if hemorrhagic or proteinaceous. T1 pre and post contrast sequences (with subtraction if available) are key. If a cystic lesion contains solid, enhancing components, there is a much higher suspicion for malignancy. T2 hyperintense

cysts are typically benign, since this indicates simple fluid, though many benign lesions will be T2 intermediate if bloody and/or proteinaceous. If only thin septations are present, or the cyst is unilocular, the lesion is also likely benign. In these cases, imaging follow-up may be beneficial to confirm benign behavior. Note that acquired thymic cysts, which are benign lesions, characteristically are multiloculated.

Diffusion weighted imaging aids in the characterization of mediastinal lesions. Cystic lesions will not demonstrate diffusion restriction unless infected. As such, a restricting lesion must either represent a solid lesion or an infected cyst. Comparison should be made to the apparent diffusion coefficient (ADC) maps, as T2 shine-through may mimic restriction on the diffusion weighted imaging (DWI) images. Simple fluid will also be bright on the ADC map, while truly restricting lesions will be dark.

Role of F18-FDG PET CT

F18-FDG PET CT has a limited role in the characterization of mediastinal cystic lesions. F18-FDG PET CT will identify hypermetabolic lesions, though numerous studies have shown low specificity as benign lesions can show similar degrees of hypermetabolism (4-7). Simple and benign cystic lesions should not demonstrate internal hypermetabolism, however it might be present in the setting of superimposed infectious or inflammatory condition. Other limitations include low spatial resolution, with the risk of small lesions not being detected despite their malignant nature as well as ametabolic malignant lesions. Specialized positron emission tomography (PET) studies with individualized radiotracers may be utilized on a case-by-case basis for metastatic lesions, neuroendocrine lesions, and other suspected malignancies.

Role of ultrasound

Transthoracic mediastinal ultrasonography can be effective in the characterization of mediastinal masses. B-flow imaging allows the visualization of flow and microbubble contrast can be safely administered to all patients (contrast-enhanced ultrasound, CEUS). The European Federation of Societies for Ultrasound in Medicine and Biology includes CEUS in its armamentarium for mediastinal imaging (8). An additional benefit of ultrasonographic imaging is its ability to be used for procedural guidance.

Simple cysts are characteristically regular, thin/

imperceptibly walled anechoic structures with posterior acoustic enhancement. Internal vascularity should be absent. Microbubble contrast, which has virtually no contraindications, may be used to further assess intralesional flow. Thick septations, solid components, internal vascularity, and irregular marginations are suspicious for malignancy.

Approach to imaging

In general, contrast-enhanced CT is the workhorse modality for characterization of virtually all mediastinal cystic lesions. In indeterminate cases, MRI can be used for troubleshooting and further characterization. Ultrasound can be utilized without risk to the patient but is limited by operator ability and depth of target lesion. F18-FDG PET CT can be used in select cases in which functional imaging may elucidate underlying lesion characteristics.

Mediastinal cysts—catalogue

The mediastinal compartment of origin can help in the differential diagnosis of cystic mediastinal lesions; however, multiple lesions can be seen involving all three compartments. For example: Malignant or infectious necrotic lymphadenopathy, lymphangiomas, hemangioma, abscess formation, hematoma, and mesothelial cysts can be found in all three compartments. The combination of typical location and imaging characteristics can often lead to a confident radiologic diagnosis without the need for tissue sampling.

Pre-vascular compartment lesions

Thymic origin lesions are the most common cystic entity found in the prevascular mediastinum (4). In general, when a simple or hemorrhagic/proteinaceous cyst without solid enhancing nodularity or thick enhancing septations are present, the most likely diagnosis is thymic cyst followed by lymphangioma.

Thymic cysts

Thymic cysts have been described as rare lesions, though reports have found them to represent up to 28.6% of mediastinal cysts and 3.7% of all mediastinal masses (9). Congenital thymic cysts are rarer than acquired thymic cysts (*Figure 1*), which tend to have a thicker wall and be multilocular secondary to inflammation or hemorrhage

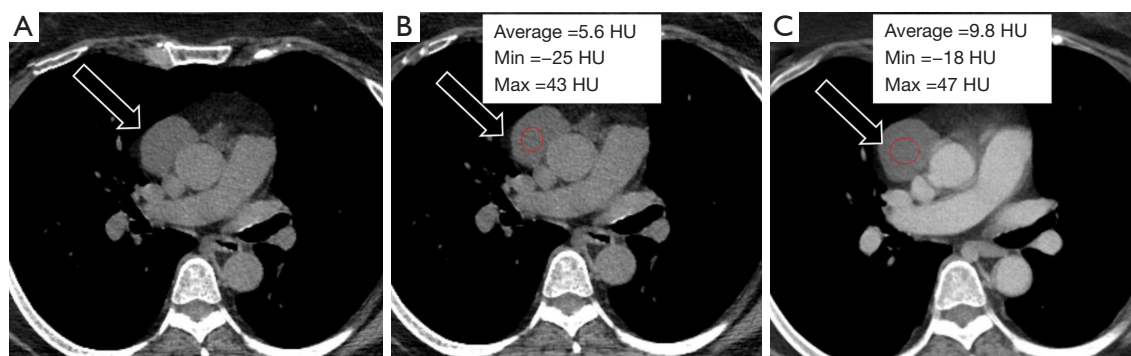


Figure 1 62-year-old female with a thymic cyst. CT imaging demonstrates a low-density lesion in the prevascular mediastinal compartment (A and B, black arrow; circle, average HU =5.6). Contrast administration subtly increases the apparent density of the lesion, but a region of interest confirms persistent fluid-attenuation of the lesion (C, black arrow and circle, average HU =9.8). This lesion was compatible with a thymic cyst on pathology. CT, computed tomography; HU, Hounsfield unit.

(Figure 2). Thymic cysts can coexist with thymic hyperplasia and thymic neoplasms. Thymic cysts are often difficult to differentiate from other mediastinal lesions. Typical imaging characteristics on CT include a prevascular midline lesion with oval or rounded shape, circumscribed with homogeneous attenuation (less than 100 HU) and that does not yield mass effect on adjacent structures. Not infrequently, these lesions have measured density over 20 HU due to hemorrhagic or proteinaceous components and can be confused for a solid mass on CT. In these cases, MRI often helps with problem solving.

Cystic thymoma

Approximately 40% of thymomas will demonstrate cystic degeneration. Like thymic cysts, a cystic lesion in the prevascular mediastinum which is oval or rounded, circumscribed and homogeneous in attenuation can represent a cystic thymoma (Figure 3). MRI is the imaging modality of choice to assess for subtle nodular components or enhancing septations which differentiate this lesion from a thymic cyst. In rare cases, thymomas may also demonstrate internal hemorrhage (Figure 4).

Approximately 90% of thymomas will demonstrate contrast enhancement on the first post-contrast sequence. Delayed post-contrast acquisitions will demonstrate enhancement in 100% of thymic neoplasms, though said enhancement may be subtle (10). For this reason, multiplanar subtraction images are recommended. Additionally, over half of thymomas will demonstrate a cystic component, though it will typically be less than the entirety of the lesion. The majority of benign thymic

cysts will demonstrate fluid signal on T2WI, some will be of low or intermediate signal. Benign cysts should not demonstrate enhancement—if present, it may be septal or rim enhancement, never internal (10).

Given the overlapping imaging characteristics of a small subset of cystic thymomas and benign thymic cysts, lesions with less than fluid signal on T2WI and non-enhancement should undergo follow-up imaging to ensure stability (11).

Mature cystic teratoma

Mature cystic teratomas and dermoid cysts are characterized by multiple tissue densities within a single mass (Figure 5). However, in many cases, these may not be readily apparent on CT imaging. MR imaging demonstrating macro or microscopic fat can aid in diagnosis (12). Multiple fat-fluid levels are highly specific (2). Gross fat is often easier to identify than microscopic fat (2).

Lymphangioma

Lymphatic malformations are often found in the prevascular compartment but can arise in all three compartments. Lymphangiomas are often indeterminate on CT, mimicking cystic neoplasms or soft tissue masses (2,13). Lymphangiomas usually present as unilocular or multilocular cystic lesion of various densities and sizes. On MRI, lymphatic lesions are typically T2 hyperintense with variable T1 signal depending on the degree of proteinaceous content. Lymphatic malformations are often septated or contain multiple grouped tubular channels, each of which may demonstrate unique T1 signal characteristics. T2 weighted sequences with fat suppression can aid in

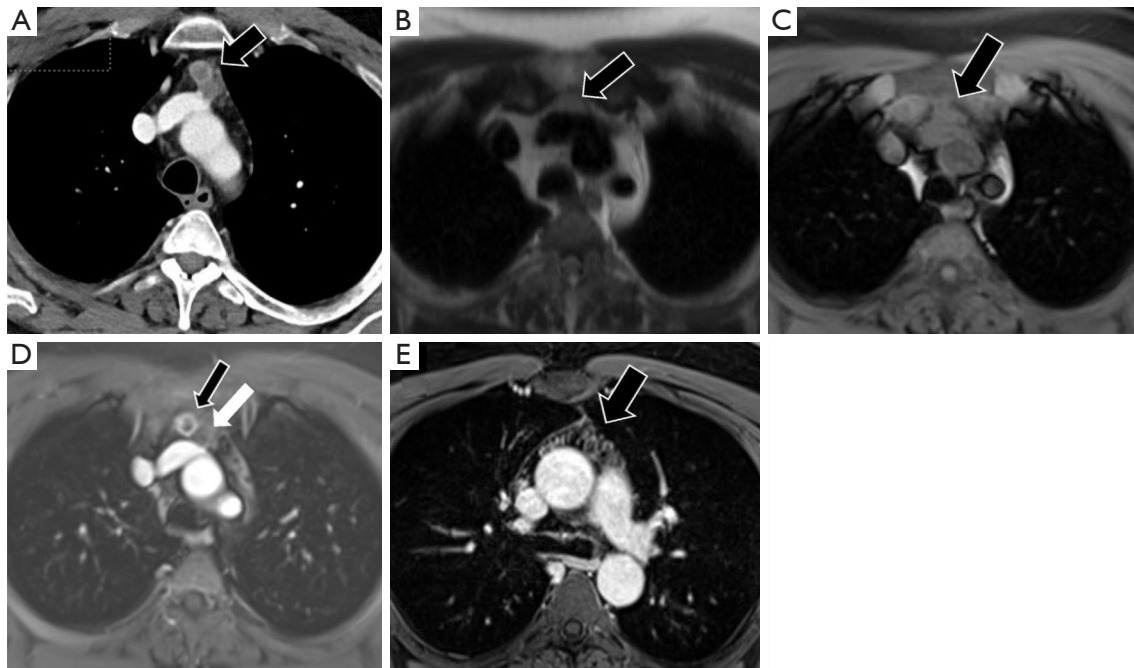


Figure 2 47-year-old male with a multiloculated (acquired) thymic cyst. CT images after the administration of contrast demonstrates multiple low-density lesions in the prevascular mediastinum (A). One of these lesions (black arrow) demonstrates peripheral high density. MRI evaluation of this lesion demonstrates intermediate to low T2 (B) and high T1 (C) signal compatible with hemorrhagic/proteinaceous components. After the administration of gadolinium, there is peripheral enhancement surrounding this lesion compatible with inflammatory changes in the capsule (D, black arrow). Other adjacent cystic lesions demonstrate simple fluid imaging characteristics and do not enhance after contrast (D, white arrow). Surrounding strands of residual thymic tissue are noted (E, black arrow). This lesion was consistent with a multiloculated thymic cyst on pathology. CT, computed tomography; MRI, magnetic resonance imaging.

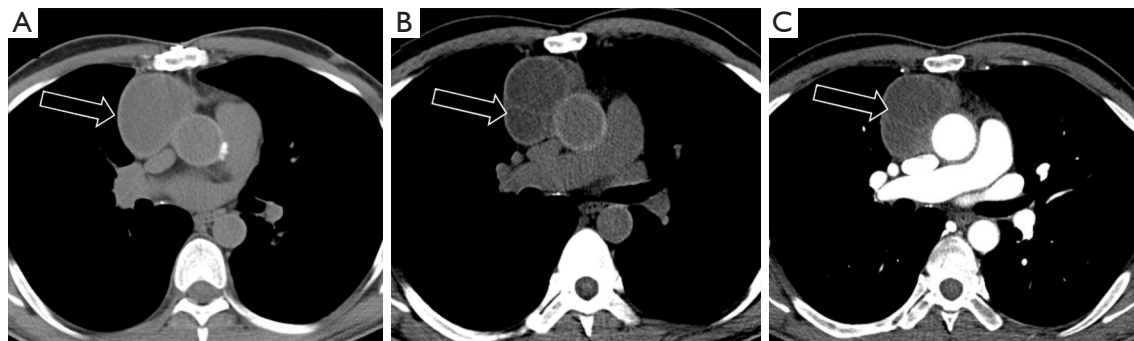


Figure 3 61-year-old male with a cystic thymoma. CT imaging demonstrates a well-circumscribed cystic lesion with minimal peripheral enhancement (A, black arrow). Thick internal septations (B, black arrow) that do not demonstrate definite enhancement (C, black arrow) are present. This is one such example in which MRI imaging would provide useful information to assess for an underlying solid mass or enhancing nodularity to corroborate cystic neoplasm. CT, computed tomography; MRI, magnetic resonance imaging.

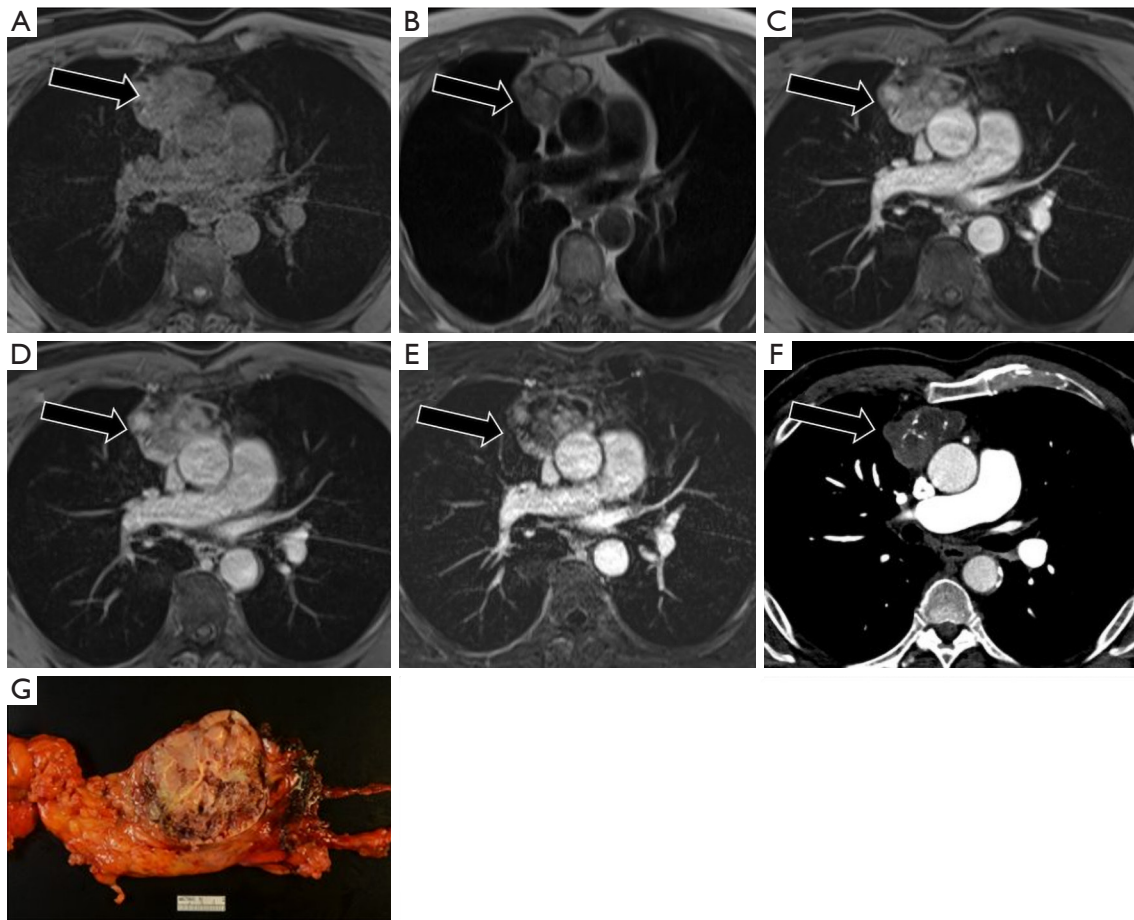


Figure 4 71-year-old-male with cystic and hemorrhagic thymoma. MRI shows a multicystic lesion (black arrow) with heterogeneous T1 signal (A), intermediate T2 signal (B), with heterogeneous internal enhancement and enhancing nodular septations (C) confirmed with delayed acquisitions (D) and subtraction (E). A contrast-enhanced CT shows enhancing internal septations (F), favoring thymic neoplasm over benign thymic cyst. Pathological specimen at time of resection (G). MRI, magnetic resonance imaging. CT, computed tomography.

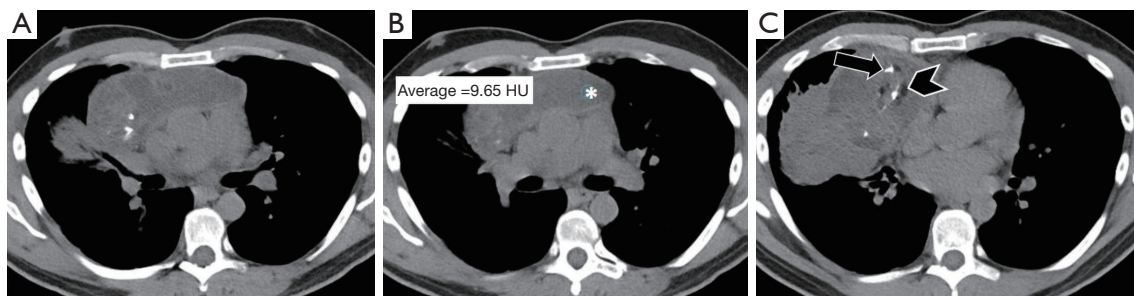


Figure 5 36-year-old male with a cystic teratoma. CT images without intravenous contrast demonstrated a large cystic and solid mass centered in the pre-vascular mediastinum (A). Note is made of areas of low-density (B, asterisk, HU =9.65; C, arrow) and high-density (C, arrowhead) compatible with fluid, fat deposition, and calcification, respectively. Pathology confirmed teratoma with cystic changes. CT, computed tomography; HU, Hounsfield unit.

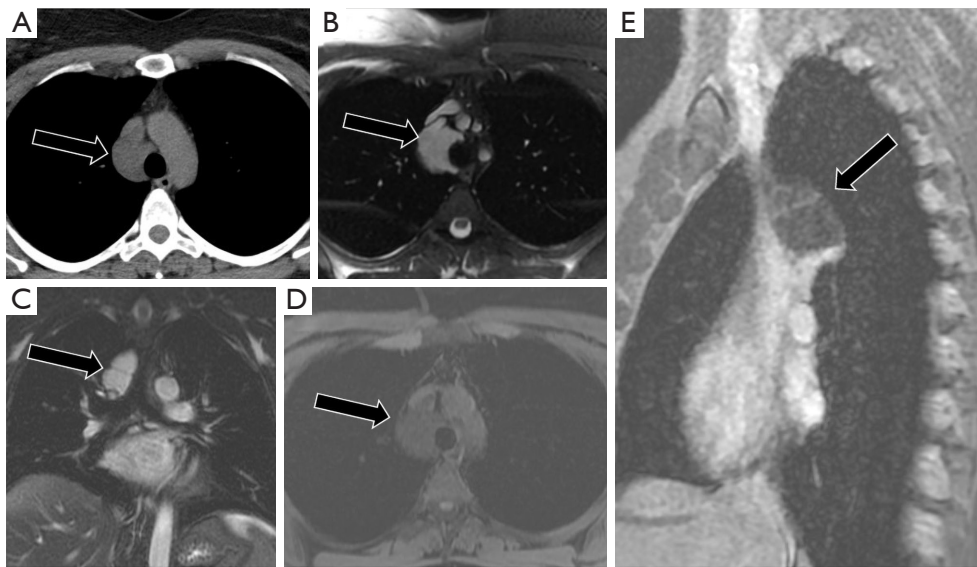


Figure 6 43-year-old female with lymphangioma. CT demonstrates a lobulated hypodense lesion in the visceral compartment (A, black arrow). MRI demonstrates a multiloculated T2W hyperintense (axial, B, black arrow; coronal, C, black arrow), T1 intermediate lesion (D, black arrow) with a thin enhancing septation (E, sagittal, black arrow), consistent with lymphangioma. CT, computed tomography; MRI, magnetic resonance imaging.

the identification of even non-dilated lymphatic channels (*Figure 6*). Lymphatic malformations may demonstrate mild enhancement secondary to contrast third spacing, or small venous channels. However, solid/nodular enhancing components should trigger further evaluation for malignancy.

Visceral compartment lesions

Foregut duplication cysts are one of the most common cystic lesions found in the visceral compartment. In this compartment, duplication cysts, pericardial cysts/diverticula, and lymphatic lesions are encountered.

Foregut duplication cysts

Foregut duplication cysts, one of the most common types of benign mediastinal cysts, can be further subdivided into neurenteric, bronchogenic, and esophageal cysts (2,14). Neurenteric cysts are persistent connections between the spinal canal and bowel. Bronchogenic cysts are abnormal ventral budding/branching of tracheobronchial tree lined by pseudostratified columnar epithelium. Esophageal cysts are outpouchings arising from the esophagus. Neurenteric cysts are more commonly found in the paravertebral compartment (see below), while bronchogenic and

esophageal cysts originate in the visceral compartment. Differentiation of these lesions, which share similar imaging characteristics, is dependent upon location and communication with the tissues of origin.

As with other cystic lesions, foregut duplication cysts demonstrate CT hypodensity, T1 hypo-intermediate intensity, and T2 intermediate-hyper intensity depending on the degree of proteinaceous debris. Duplication cysts may become infected after intervention. In such cases, intermediate signal and thicker rim enhancement may be seen (*Figure 7*).

Pericardial cysts/diverticula

Pericardial cysts are functionally mesothelial cysts of the pericardium, most commonly found in the cardiophrenic angles (right greater than left). Both pericardial cysts and diverticula are caused by abnormal fusion of the mesenchymal lacunae, though diverticula retain communication with the pericardial space while cysts are isolated. Pericardial diverticula may change in size and shape with positioning, while cysts may grow slowly over time. Pericardial cysts account for up to 6% of all mediastinal masses and 33% of mediastinal cysts (15,16). Pericardial cysts are typically single, simple cysts—well-defined, low-density lesions on CT (30–40 HU), homogeneous T1 hypo/

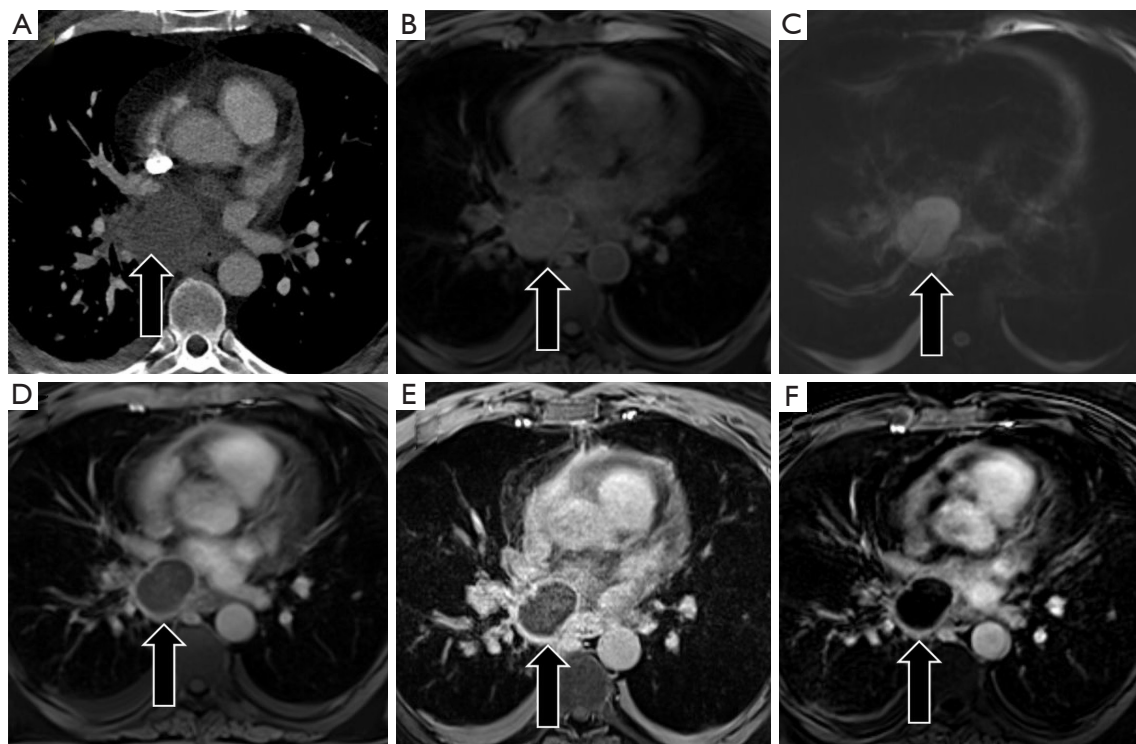


Figure 7 In this 47-year-old male, an esophageal duplication cyst underwent biopsy and subsequently developed an infection. Contrast-enhanced CT demonstrates a non-enhancing, intermediate density lesion in the visceral compartment (A, black arrow). MRI demonstrates intermediate to high T1 (B, black arrow) and high T2 signal (C, black arrow) within the lesion. After the intravenous administration of gadolinium, there is a peripheral capsular enhancement without internal septations or solid enhancing component (D and delayed acquisition E, black arrow). This is confirmed on subtraction images (F, black arrow). CT, computed tomography; MRI, magnetic resonance imaging.

T2 hyper (unless proteinaceous) (*Figure 8*).

Pericardial abscess/post-interventional collections

Abscesses can rarely arise in the pericardium, typically after surgical or percutaneous intervention. These lesions can mimic other cystic neoplasms.

Like abscesses in other anatomic locations, pericardial abscesses will be characterized by a rim-enhancing fluid collection that demonstrates T1 intermediate or low signal and T2 intermediate or high signal. Diffusion restriction is characteristic. A history of recent pericardial intervention is beneficial in confirming the diagnosis (*Figure 9*).

Mycetoma

In addition to mediastinal abscesses, other infectious collections may be encountered in the mediastinum. Fungal mycetomas demonstrate similar imaging characteristics to abscesses (*Figure 10*). A thorough clinical history with focus upon exposure history and potential causes of immunocompromise can be beneficial. For example, the

illustrated case was of a patient with histoplasmosis with immunocompromise secondary to hematologic malignancy and a history of spelunking in endemic regions.

Paravertebral compartment lesions

Paravertebral compartment lesions are most likely neurogenic in origin (17). Cystic lesions of neurogenic origin include meningocele, cystic schwannoma, and neurenteric cysts.

Meningocele

Meningoceles are anomalous paravertebral cystic masses that result from leptomeningeal herniation into an intervertebral foramen or a vertebral body defect. In the former, the intervertebral foramen can be widened. Meningoceles will follow cerebrospinal fluid (CSF) intensity on MRI sequences—T1WI hypointensity and T2WI hyperintensity (18). Often, cystic neurogenic lesions can mimic meningoceles. However, communication with the

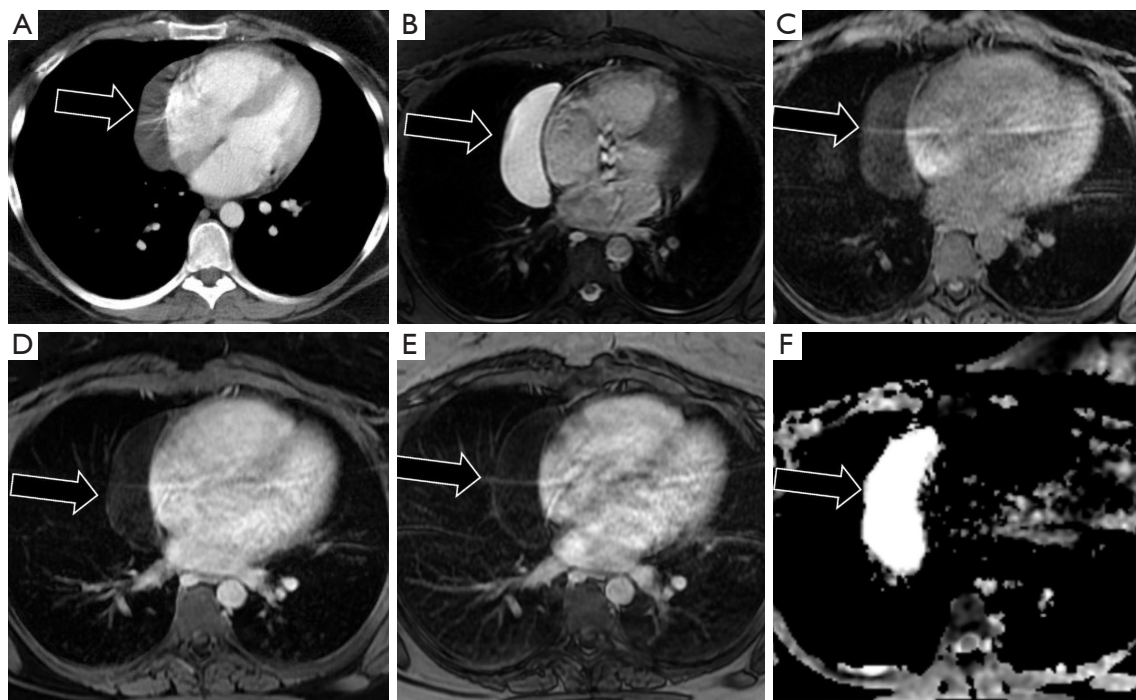


Figure 8 26-year-old female with pericardial cyst. CT imaging (black arrow) demonstrates a fluid density lesion along the right cardiac border (A), corresponding to T2W hyperintensity (B) and T1W hypointensity (C). The lesion does not demonstrate gadolinium enhancement (D), confirmed on delayed acquisitions (E). ADC maps demonstrate increased diffusivity (F). The location and imaging findings are confirmatory for pericardial cyst. CT, computed tomography; ADC, apparent diffusion coefficient.

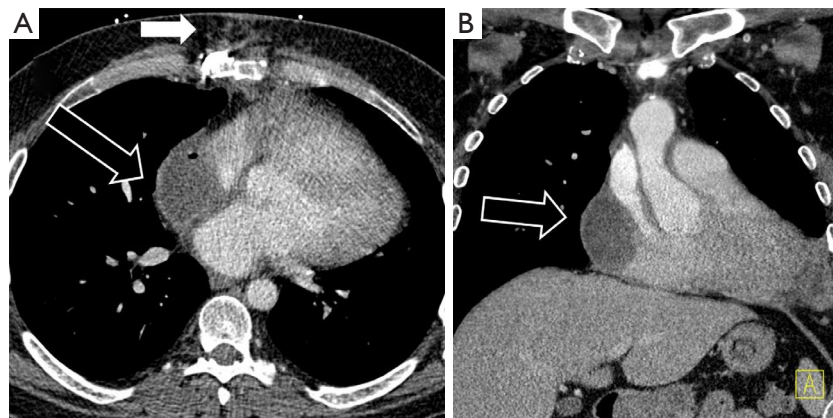


Figure 9 29-year-old male status post heart transplant with a pericardial abscess. Axial CT image after the administration of contrast demonstrated inflammatory changes in the sternum compatible with known infection (A, white arrow). A loculated pocket of fluid with small amount of gas is noted in the pericardium, immediately adjacent to the right atrium, compatible with intrapericardial abscess formation (A, black arrow; B, black arrow). CT, computed tomography.

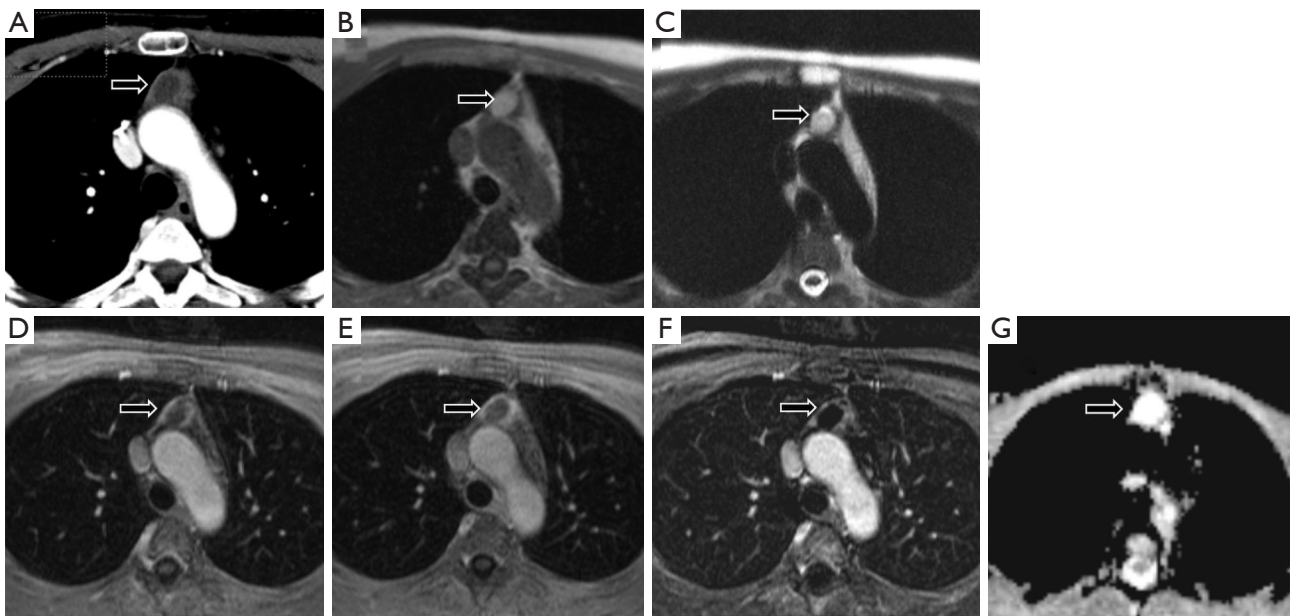


Figure 10 A 37-year-old male with negative tissue cultures but tissue PCR consistent with histoplasmosis. A contrast-enhanced CT demonstrates a thick walled, hypodense collection in the prevascular compartment (A, black arrow). MRI demonstrated (black arrow) a high T1 (B), high T2 (C) signal lesion with peripheral enhancement after the administration of gadolinium (D; delayed acquisition E). Subtraction images confirm the lack of internal enhancement (F). ADC images demonstrate increased diffusivity (G). PCR, polymerase chain reaction; CT, computed tomography; MRI, magnetic resonance imaging; ADC, apparent diffusion coefficient.

the cal sac confirms a diagnosis of meningocele (14).

Cystic schwannoma

Schwannomas are benign neoplasms arising from peripheral nerve sheaths. MRI is helpful in identifying the lesion and characterizing extension through the neuroforamen. Schwannomas are typically T2 hyperintense with small, ring-like hypointensities representing nerve fascicles. Schwannomas have a characteristic pattern of heterogeneous contrast enhancement. Cystic degeneration leads to areas of very bright T2 signal (*Figure 11*). Contrast administration can help differentiate cystic degeneration of a Schwannoma from other cystic lesions, as the underlying Schwannoma will retain its heterogeneous enhancement pattern (14).

Neurenteric cyst

Neurenteric cysts represent a notochordal defect in which a persistent connection between the bowels and spinal canal is present. Most commonly in the posterior mediastinum, right hemithorax, and above the carina, these typically present as ventral paravertebral cysts with accompanying vertebral abnormalities, particularly of the thoracic spine. Signal characteristics are similar to meningocele (following

CSF). If the connection to the bowel is patent, air or air-fluid levels may be seen (18).

Mullerian cyst (cysts of Hattori)

First characterized by Hattori in 2005, müllerian cysts are rare paravertebral cystic lesions in the T3–T8 region (19). Typically found in women aged 40–60 with concomitant gynecologic pathology, these lesions are thought to arise due to müllerianosis, a process by which müllerian tissues are developmentally misplaced (20). A cyst of Hattori is a singular, well-defined fluid attenuation lesion without enhancement that does not communicate with other structures, usually measuring less than 10 cm. Histopathologically, these lesions resemble fallopian tissue and display estrogen and progesterone receptor positivity. Surgical excision is often the preferred treatment given a presumed risk of malignant transformation (21).

Cyst-like lesions

Mediastinal pancreatic pseudocyst

A rare complication of acute and chronic pancreatitis is mediastinal extension of a pancreatic pseudocyst,

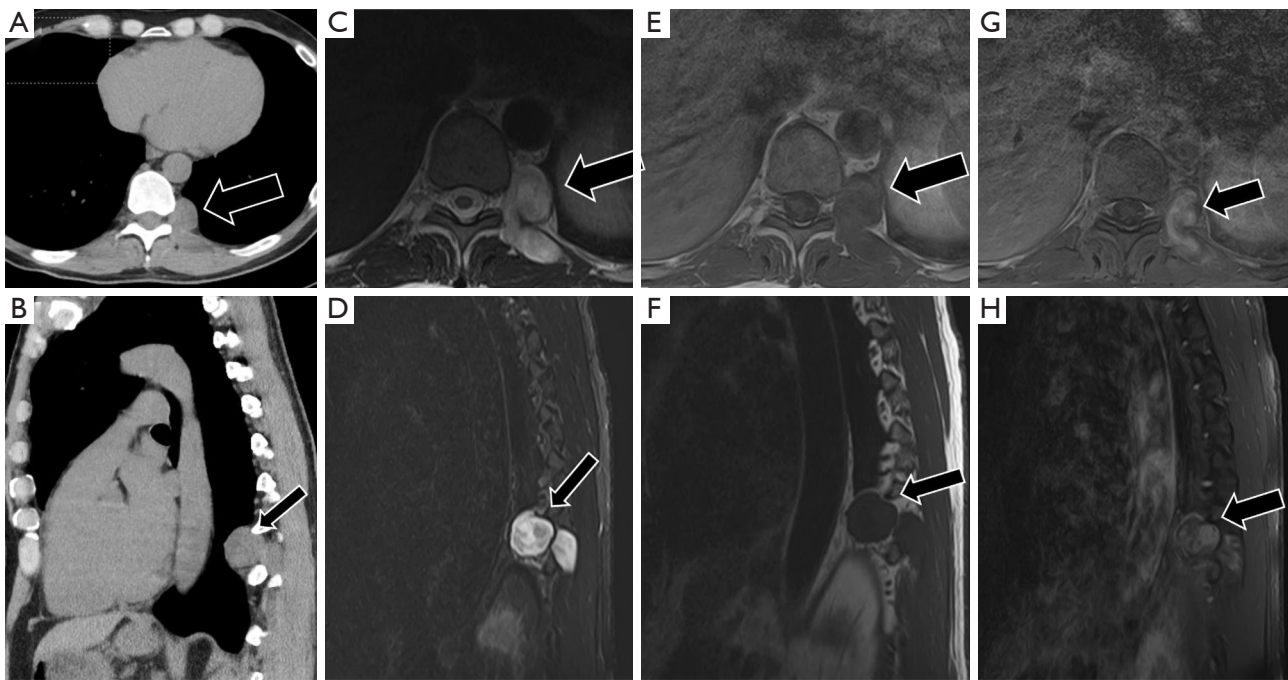


Figure 11 55-year-old male with cystic degeneration of a schwannoma. CT imaging demonstrates a soft-tissue density lesion (black arrow) arising in the paravertebral compartment (axial, A; sagittal, B). MRI imaging (black arrow) demonstrates a high T2 (axial, C; sagittal, D), intermediate T1 signal (axial, E; sagittal, F) lesion with extension to the posterior paraspinal musculature. Heterogeneous contrast enhancement is seen after the administration of gadolinium (axial, G; sagittal, H). Overall imaging findings compatible with cystic degeneration of a schwannoma. Also note the lack of direct communication with the thecal sac. CT, computed tomography; MRI, magnetic resonance imaging.

most commonly into the posterior mediastinum via the esophageal hiatus. Imaging characteristics will mirror those of abdominal pancreatic pseudocysts, typically thin-walled fluid collections, or alternatively, thick-walled, rim enhancing fluid collections. Communication with the abdominal cavity is typically, but not always, seen. Another potential route of communication and extension is a Morgagni hernia (congenital anterior diaphragmatic defect). Accurate diagnosis is critical as treatment for symptomatic lesions involves endoscopic-guided drainage with surgical resection necessary for most recurrent pseudocysts (22-26).

Ascending ascites via esophageal hiatus

Similar to pancreatic pseudocyst formation with mediastinal extension, intra-abdominal fluid contrast can ascend through the esophageal hiatus into the visceral mediastinum and simulate a cystic lesion (*Figure 12*). Fluctuation in shape and the presence of a concomitant sliding-type hiatal hernia help to confirm the diagnosis. Ascending ascites should follow the signal characteristics of the associated abdominal

fluid and will not enhance.

Normal variants

Cysterna chyli

The cisterna chyli is a normal anatomical variant, representing a saccular dilatation of the retrocrural lymphatics as they ascend into the mediastinum. The cisterna chyli is often found immediately to the right of the aorta and can easily be mistaken for a cystic lesion. The characteristic location, morphology, and low attenuation on CT allow for confident identification (*Figure 13*). On MRI, the signal follows that of simple fluid (T1 hypointense, T2 hyperintense, no restriction).

Thymic hyperplasia

Thymic hyperplasia can be identified on CT imaging due to its characteristic location, triangular shape, and stippled appearance. However, in equivocal cases, in and opposed phase MR imaging can be used to demonstrate intracellular

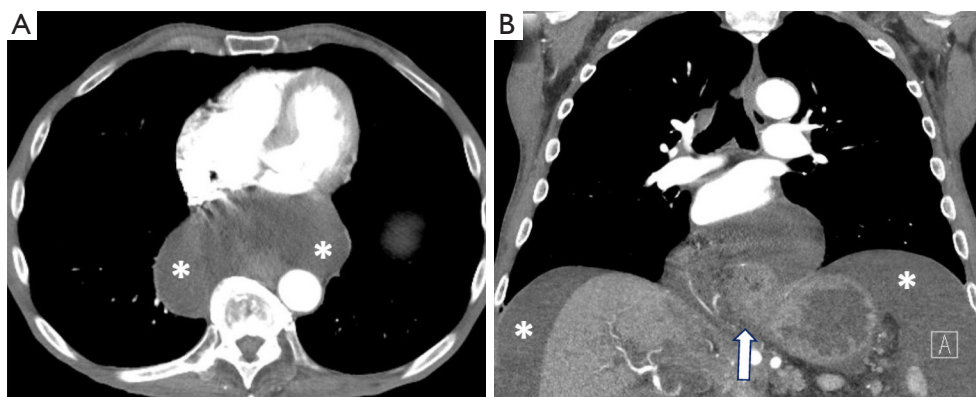


Figure 12 76-year-old male with ascending ascites. CT imaging demonstrates ill-defined hypoattenuation centered in the visceral compartment of the mediastinum (A, asterisks). No enhancement is present (A). Coronal image demonstrates the fluid is in continuity with abdominal ascites (B, asterisks). Note the hiatal hernia, a common finding in patients with ascending mediastinal ascites (B, white arrow). The hiatal hernia can also be faintly recognized in the selected axial image. CT, computed tomography.

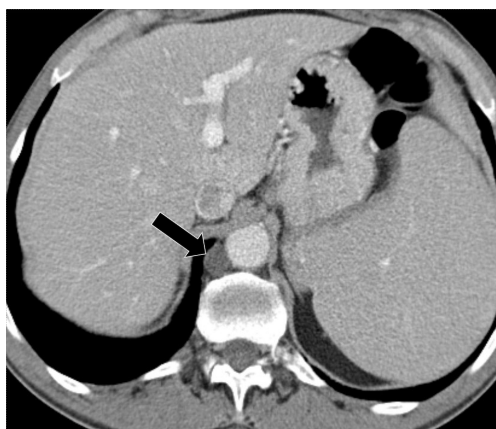


Figure 13 80-year-old male. CT image demonstrates a classic appearance of the cisterna chyli, a fluid-attenuation lesion located immediately to the right of the aorta at its diaphragmatic hiatus (black arrow). CT, computed tomography.

lipid, adding confidence to a diagnosis of thymic hyperplasia (12,27). One quantitative measure that may be used to differentiate benign from malignant prevascular (anterior) mediastinal thymic masses is the signal intensity index (SII), a ratio representing the percentage signal drop-off in out of phase imaging $[(\text{Thymus SI IP} - \text{Thymus SI OP}) / \text{Thymus SI IP} \times 100\%]$. Values greater than 9%, typically 28–65%, were only seen in thymic hyperplasia (2,27,28). Another quantitative measure to differentiate benign versus malignant pre-vascular thymic lesions is the quantification

of the chemical shift ratio (CSR) (27). A $\text{CSR} \leq 0.7$ is consistent with normal or hyperplastic thymus, while a $\text{CSR} \geq 1.0$ is indicative of thymic neoplasm in most cases (0.8 and 0.9 are indeterminate values). The formula to calculate CSR is as follows: $\text{CSR} = \text{OP SI thymus} / \text{OP SI paraspinal muscle} / \text{IP SI thymus} / \text{IP SI paraspinal muscle}$. Other studies have identified diffusion restriction as a predictor of malignancy, with some establishing quantitative ADC cutoffs that demonstrate 81% sensitivity. Lastly, contrast enhancement kinetics may be able to aid in differentiating low grade neoplasms from more aggressive lesions (2).

Thoracic duct cysts

Thoracic duct cysts can arise along its entire course, from the cisterna chyli to the supraclavicular region. Mediastinal thoracic duct cysts are extremely rare, accounting for only a few case reports in the literature (29). These lesions will follow signal characteristics similar to the cisterna chyli and lymphatic tissues, as above.

Pericardial recess

Fluid-filled pericardial recesses can be confused with mediastinal cystic lesions. Anatomical knowledge and imaging appearance of the pericardial recesses is needed to avoid confusion. Important pericardial recesses to mention include the posterior pericardial recess (blind ending extension of the oblique sinus) which is located immediately above the left atrium to the right of midline, and the pulmonary venous recesses which surround the pulmonary

veins near their attachment to the left atrium (30).

Conclusions

The imaging of cystic mediastinal lesions remains a diagnostic challenge. Location and imaging characteristics can often confirm a diagnosis without the need for tissue sampling. CT, MRI, and US each offer unique strengths and weaknesses. CT is often the first-line modality used in identification and characterization, MRI with T1 weighted pre and post contrast, T2 weighted, and diffusion-weighted sequences is a critical problem-solving tool, and ultrasonography useful in real-time characterization and procedural guidance. Findings suggestive of malignancy include enhancing solid or nodular components, thick vascular septations, and diffusion restriction. In equivocal or atypical cases, short-term follow-up imaging may be considered to reduce the number of unnecessary biopsies and/or resections.

Acknowledgments

Funding: None.

Footnote

Provenance and Peer Review: This article was commissioned by the Guest Editor (Nestor Villamizar) for the series “Mediastinal Cysts” published in *Mediastinum*. The article has undergone external peer review.

Peer Review File: Available at <https://med.amegroups.com/article/view/10.21037/med-22-31/prf>

Conflicts of Interest: Both authors have completed the ICMJE uniform disclosure form (available at <https://med.amegroups.com/article/view/10.21037/med-22-31/coif>). The series “Mediastinal Cysts” was commissioned by the editorial office without any funding or sponsorship. The authors have no other conflicts of interest to declare.

Ethical Statement: The authors are accountable for all aspects of the work in ensuring that questions related to the accuracy or integrity of any part of the work are appropriately investigated and resolved.

Open Access Statement: This is an Open Access article distributed in accordance with the Creative Commons

Attribution-NonCommercial-NoDerivs 4.0 International License (CC BY-NC-ND 4.0), which permits the non-commercial replication and distribution of the article with the strict proviso that no changes or edits are made and the original work is properly cited (including links to both the formal publication through the relevant DOI and the license). See: <https://creativecommons.org/licenses/by-nc-nd/4.0/>.

References

1. Carter BW, Tomiyama N, Bhora FY, et al. A modern definition of mediastinal compartments. *J Thorac Oncol* 2014;9:S97-101.
2. Carter BW, Betancourt SL, Benveniste MF. MR Imaging of Mediastinal Masses. *Top Magn Reson Imaging* 2017;26:153-65.
3. Raptis CA, McWilliams SR, Ratkowski KL, et al. Mediastinal and Pleural MR Imaging: Practical Approach for Daily Practice. *Radiographics* 2018;38:37-55.
4. Carter BW, Benveniste MF, Marom EM. Diagnostic approach to the anterior/prevascular mediastinum for radiologists. *Mediastinum* 2019;3:18.
5. Tatci E, Ozmen O, Dadali Y, et al. The role of FDG PET/CT in evaluation of mediastinal masses and neurogenic tumors of chest wall. *Int J Clin Exp Med* 2015;8:11146-52.
6. Jerushalmi J, Frenkel A, Bar-Shalom R, et al. Physiologic thymic uptake of 18F-FDG in children and young adults: a PET/CT evaluation of incidence, patterns, and relationship to treatment. *J Nucl Med* 2009;50:849-53.
7. Kubota K, Yamada S, Kondo T, et al. PET imaging of primary mediastinal tumours. *Br J Cancer* 1996;73:882-6.
8. Trenker C, Dietrich CF, Holland A, et al. Mediastinal Masses in Contrast-Enhanced Ultrasound - Retrospective Analysis of 58 Cases. *J Ultrasound Med* 2021;40:1023-30.
9. Takeda S, Miyoshi S, Minami M, et al. Clinical spectrum of mediastinal cysts. *Chest* 2003;124:125-32.
10. Hammer MM, Barile M, Bryson W, et al. Errors in Interpretation of Magnetic Resonance Imaging for Thymic Lesions. *J Thorac Imaging* 2019;34:351-5.
11. McInnis MC, Flores EJ, Shepard JA, et al. Pitfalls in the Imaging and Interpretation of Benign Thymic Lesions: How Thymic MRI Can Help. *AJR Am J Roentgenol* 2016;206:W1-8.
12. Madan R, Ratanaprasatporn L, Ratanaprasatporn L, et al. Cystic mediastinal masses and the role of MRI. *Clin Imaging* 2018;50:68-77.
13. Jeung MY, Gasser B, Gangi A, et al. Imaging of cystic masses of the mediastinum. *Radiographics* 2002;22 Spec

- No:S79-93.
14. Park JW, Jeong WG, Lee JE, et al. Pictorial Review of Mediastinal Masses with an Emphasis on Magnetic Resonance Imaging. *Korean J Radiol* 2021;22:139-54.
 15. Khayata M, Alkharabsheh S, Shah NP, et al. Pericardial Cysts: a Contemporary Comprehensive Review. *Curr Cardiol Rep* 2019;21:64.
 16. Tower-Rader A, Kwon D. Pericardial Masses, Cysts and Diverticula: A Comprehensive Review Using Multimodality Imaging. *Prog Cardiovasc Dis* 2017;59:389-97.
 17. Strollo DC, Rosado-de-Christenson ML, Jett JR. Primary mediastinal tumors: part II. Tumors of the middle and posterior mediastinum. *Chest* 1997;112:1344-57.
 18. Vargas D, Suby-Long T, Restrepo CS. Cystic Lesions of the Mediastinum. *Semin Ultrasound CT MR* 2016;37:212-22.
 19. Hattori H. Ciliated cyst of probable müllerian origin arising in the posterior mediastinum. *Virchows Arch* 2005;446:82-4.
 20. Batt RE, Mhawech-Fauceglia P, Odunsi K, et al. Pathogenesis of mediastinal paravertebral müllerian cysts of Hattori: developmental endosalpingiosis-müllerianosis. *Int J Gynecol Pathol* 2010;29:546-51.
 21. Saad Abdalla Al-Zawi A, Idaewor P, Asaad A, et al. Posterior Mediastinal Paravertebral Müllerian cyst (cyst of Hattori): literature review. *Adv Respir Med* 2020;88:134-41.
 22. Bhasin DK, Rana SS, Rao C, et al. Clinical presentation, radiological features, and endoscopic management of mediastinal pseudocysts: experience of a decade. *Gastrointest Endosc* 2012;76:1056-60.
 23. Gee W, Foster ED, Doohen DJ. Mediastinal pancreatic pseudocyst. *Ann Surg* 1969;169:420-4.
 24. Sadat U, Jah A, Huguet E. Mediastinal extension of a complicated pancreatic pseudocyst; a case report and literature review. *J Med Case Rep* 2007;1:12.
 25. Vitellas C, Mangeb IB, Regalado L, et al. Mediastinal Extension of a Pancreatic Pseudocyst: A Rare Intrathoracic Complication of Pancreatitis. *Case Rep Radiol* 2021;2021:1919550.
 26. Weinfeld A, Kaplan JO. Mediastinal pancreatic pseudocyst. *Gastrointest Radiol* 1979;4:343-7.
 27. Inaoka T, Takahashi K, Mineta M, et al. Thymic hyperplasia and thymus gland tumors: differentiation with chemical shift MR imaging. *Radiology* 2007;243:869-76.
 28. Priola AM, Priola SM, Ciccone G, et al. Differentiation of rebound and lymphoid thymic hyperplasia from anterior mediastinal tumors with dual-echo chemical-shift MR imaging in adulthood: reliability of the chemical-shift ratio and signal intensity index. *Radiology* 2015;274:238-49.
 29. Mortman KD. Mediastinal thoracic duct cyst. *Ann Thorac Surg* 2009;88:2006-8.
 30. Truong MT, Erasmus JJ, Gladish GW, et al. Anatomy of pericardial recesses on multidetector CT: implications for oncologic imaging. *AJR Am J Roentgenol* 2003;181:1109-13.

doi: 10.21037/med-22-31

Cite this article as: Shah A, Rojas CA. Imaging modalities (MRI, CT, PET/CT), indications, differential diagnosis and imaging characteristics of cystic mediastinal masses: a review. *Mediastinum* 2023;7:3.